

All-optical attoclock: accessing exahertz dynamics of optical tunnelling through terahertz emission

I. Babushkin,^{1,2} A. J. Galan,² A. Husakou,² F. Morales,² A. Demircan,^{1,3} J. R. C. Andrade,^{1,3} U. Morgner,^{1,3} and M. Ivanov²

¹*Institute for Quantum Optics, Leibniz Universität Hannover, Welfengarten 1, 30167 Hannover, Germany*

²*Max Born Institute, Max Born Str. 2a, 12489 Berlin, Germany*

³*Hannover Centre for optical Technologies, Nienburger Str. 17, 30167 Hannover, Germany*

The hot debate regarding attosecond dynamics of optical tunneling has, so far, been focused on the presence, or absence, of time delays associated to the electron tunnelling through the classically forbidden region during atomic ionization in intense infrared laser fields. Strong theoretical and experimental arguments have been put forward to advocate the polar opposite points of view. The underlying dynamics are richer. Here we propose to use the nonlinear optical responses of the tunnelling electrons to tailored light fields to track these dynamics in full complexity. Using the combination of single-color and two-color fields, we resolve not only ionization delays, but also temporal re-shaping and spatial re-focusing of the tunnelling wavepacket as it emerges from the classically forbidden region. Access to these details of the dynamics is facilitated by the near-instantaneous nature of the nonlinear optical response driven by ionization, and by using tailored laser pulses to induce this response. Our work introduces a new type of attoclock for optical tunnelling, one that is based on measuring light rather than photo-electrons. Our conclusions suggest a possible middle ground between the two conflicting points of view.

Ionization processes induced by strong fields are a key resource in attosecond science [1–4] enabling high harmonic spectroscopy, attosecond pulse generation and many other applications. In recent years there has also been a breakthrough in our understanding of electron dynamics in atoms and molecules in strong fields [5–11]. Even taking the simplest possible example of the hydrogen atom, whose levels can be quantified fully analytically, the process of ionization gives rise to extremely rich dynamics which include, for instance, the low-energy structures or interferences of the electron wavepackets [5, 7, 9]. Of course, more effects are to be expected in the case of multielectron atoms, simple and complex molecules and solids [6, 8, 11]. Many of these phenomena are based on extremely high harmonics emitted by the electrons as they return to the parent ion (the process can be described as a bound-continuum-bound transition). The typical frequencies emitted in this case are in the XUV range. But even if the electron does not return back to the core, it nevertheless emits radiation

(bound-continuum transitions) which is often referred to as “Brunel harmonics” [12–15]. In the case of a two-color (or single-color but few-cycle) pump, there is a 0th order Brunel harmonic which lies in the terahertz (THz) frequency range [16–19]. The analysis of these ultrashort THz pulses has been used for spectroscopy, for instance to unveil the electron dynamics in solids [20–22].

Detecting electrons delivers valuable information about the ionization dynamics [9, 23–26]. Key examples are the attosecond electron streaking techniques [27], one of which being the attoclock [23, 24, 26, 28–30]. In the attoclock procedure, one ionizes electrons with a strong elliptically polarized few-cycle optical pulse and detects them away from the atom. The rotating field provides a moving “clock hand”, so that the electrons escaping the atom at different times are mapped to different angles of detection (see Fig. 1a). Such observations revealed a shift between the maximum of the electron distribution and that of the pump field’s polarization ellipse which can be interpreted as a temporal delay during the ionization process, usually lying in the range of tens to hundred of attoseconds. The nature of this delay is highly controversial and is a subject of active discussions [26, 29, 31–39]. Besides the several existing approaches to define the tunneling time, on its way to the detector the electron wavepacket experiences the influence of the external electric field, the core potential and also the quantum-mechanical diffusion. This complicates the interpretation of the measurements as it is necessary to implement a reconstruction of the electron dynamics until detection. Approaches based on resolving HHG spectra (rather than the electrons themselves) also exist [40–42]. However, each XUV harmonic has its own ionization time and even this information is highly entangled in the whole spectrum. Nonetheless, several works [29, 36, 42] have surfaced to tackle this reconstruction from the XUV light, or to make it simpler using a two-color-pulse attoclock [30]. Yet, the reconstruction strategies that allow to disentangle the electron birth information from the electron propagation dynamics in the continuum are still rather complex. The attempts to characterize the ionization distributions beyond the ionization time are only rarely considered [29], almost exclusively in the context of ionization of aligned molecules [43, 44] although it is clear that the complex ionization dynamics must be described by more than a single quantity.

In general, questioning to which extent the measurement of electron velocities at distant detectors (meaning large propagation times) are able to uncover all its dynamics on the way to the detector is still valid. Electron-based attoclocks require extremely complicated bulky setups (COLTRIMS, VMIS) and nearly single-cycle pulses. The available precision of $\sim 1^\circ$ for the angular electronic distributions (translated to ~ 10 as) is a few orders of magnitude lower than the one for light polarimeters, for both optical and THz frequencies [45–47] which is around 0.01° and below. Furthermore, in solids, the free propagation paths of electrons are in the range of nanometers [48] thus making the attoclock experiments challenging. The time-of-flight based electron streaking techniques in solids [49] exist, but delay obtained in this way are even more difficult to interpret than the ones in gases [49, 50].

Here, we present an all-optical approach to extract the full information of the ultrafast dynamics that occur during strong field ionization. We show that very low-frequency Brunel harmonics can provide immediate, *in-situ* [51] attoclock information, since they start being produced throughout the electron ionization process. Somewhat paradoxically, although the lowest frequencies can be far from resolving the attosecond timescale, the deep-subcycle details of the ionization process are nonetheless fingerprinted in their polarization state. In particular, the ionization delay is imprinted in the 0th order Brunel harmonic whereas the reshaping of the ionization distribution is encoded in the 3rd one. Using light instead of electrons paves a way to greatly extend the attoclock applicability (for instance to solids) as well as to boost its precision to the sub-attosecond range.

RESULTS

We consider atomic hydrogen as a paradigmatic case since it captures all of the relevant physics while being simple and amenable to theory. As a first step, we discuss results from an atom in an electromagnetic field which is composed of a circularly polarized strong infrared pump with frequency ω_0 and its co-rotating second harmonic $2\omega_0$, both having the same amplitude, as shown in Fig. 1b. Under these conditions, the atomic response spectrum contains all harmonics $n\omega_0$, $n = 0, 1, 2, \dots$, which rotate in the same direction. The signal close to the 0th harmonic, however, is almost linearly polarized. This signal, typically, has a maximum in the terahertz (THz) frequency range but can be as broad as 100 THz and hence observable as well up to the mid-infrared. One of the main results of this Letter is that the polarization direction of the 0th order harmonic identifies the ionization delay τ : the rotation angle ϕ with respect to the y -axis of Fig. 1b is $\phi = \omega_0\tau$. This property is preserved throughout the 0th harmonic signal, extending up to the optical frequencies.

Furthermore, we show that besides the ionization delay, more details about the ionization dynamics can be obtained if higher-order Brunel harmonics are considered. By using a single-color elliptically polarized field (see Fig. 1c), we show that the polarization state (ellipticity and polarization direction) of the 3rd Brunel harmonic encodes the attosecond reshaping of the ionization distribution with respect to the field maxima.

High order harmonics appear as a consequence of three different contributing mechanisms: bound-free transitions (Brunel radiation), bound-bound transitions (non-resonant frequency mixing) and bound-free-bound transitions (Lewenstein harmonics). The weight of each of these mechanisms varies for different harmonics. For our approach, we seek harmonics generated predominantly by Brunel radiation. Fig. 2a,c shows the contribution of each of these mechanisms as a function of the harmonic order for a co-rotating 800-400 nm bicircular driver and an 800 nm single-color elliptical driver ($\epsilon=0.6$), respectively.

The black circles are calculations using the time-dependent Schrödinger equation (TDSE) described in [52] for the hydrogen atom, which mimics the harmonic response that would be experimentally observed, and where naturally all of the three mechanisms mentioned are included. The red squares are calculations using the TDSE as well but for a Yukawa potential, chosen so that it contains a single bound state while retaining the same ionization potential as the hydrogen atom (see Methods). This calculation permits to both estimate the contribution of bound-bound transitions, which are absent in the Yukawa potential, and calibrate the optical attoclock in a similar way to what was done in [26]. The blue triangles are computed using the Drude model, where the response is calculated as the product of the electric field $\mathbf{E}(t)$ and the free electron density $\rho(t)$: $\mathbf{E}_r(t) = \mathbf{E}(t)\rho(t)$ (see Methods). The latter gives us a simple estimation of the impact of the bound-continuum transitions. Finally, the gray crosses in Fig. 2a,c give an estimation of the strength of the bound-bound transitions, where now the response is calculated as $\mathbf{E}_r = \chi^{(3)}|\mathbf{E}|^2\mathbf{E}$, being $\chi^{(3)}$ the corresponding nonlinearity coefficient obtained from Ref. [53]: $\chi^{(3)} = 0.8 \times 10^{-20}$ W/cm².

Based on the comparison of the different calculations we are able to separate the harmonic spectra into three regions, depending on the dominant transition mechanism. Region I (Fig. 2a,c blue shading) corresponds to the linear response, and the polarization state of the harmonics is determined solely by the pump field. In region II (Fig. 2a,c green shading), the Brunel mechanism (bound-free transitions), given by the Drude model, dominates over the bound-bound and bound-continuum-bound transitions. This region contains the 0th and 3rd harmonics in both the two-color and single-color case. The influence of bound-bound transitions in region II, as well as in the other two regions, which is estimated

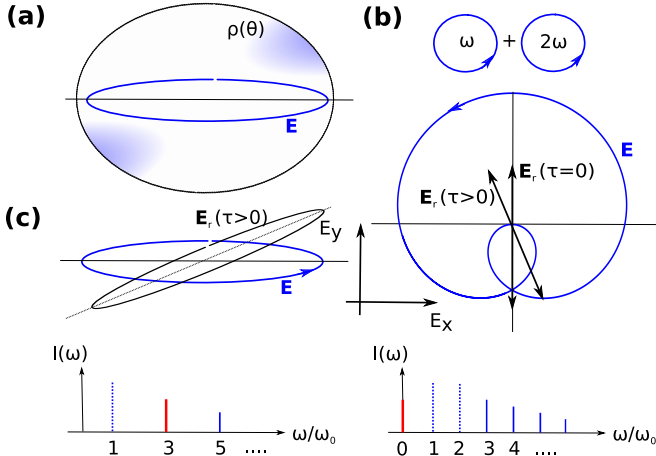


FIG. 1. Ionization dynamics and delay observed by detecting ionized electrons (a) and the Brunel harmonics (b,c) using two (b) and single-color (c) fields. In (a), the electrons ionized by the elliptically polarized electric field (blue line) are detected in an angular(θ)-resolved way, giving the electron density $\rho(\theta)$ (blue gradient) at a remote detector (black line). It has the maxima shifted from the extrema of the electric field due to a nonzero ionization delay time τ , providing the “attoclock” measurement of the ionization delay. In (b), this delay is probed, instead of electrons, by the 0th-order Brunel radiation \mathbf{E}_r in a two-color field \mathbf{E} . The Brunel radiation is linearly polarized and, in the presence of a nonzero ionization delay, rotated by the angle $\tau\omega_0$. In (c), a single-color elliptically polarized pump \mathbf{E} produces the 3rd Brunel harmonic which contains in its polarization state (ellipticity and polarization direction) the details about the sub-cycle dynamics of the ionization process. The spectra below show schematically the harmonic structure of the atomic response. With dashed lines the pump is shown and the red line indicates the harmonics of interest for the analysis.

directly from the $\chi^{(3)}$ model, is several orders of magnitude smaller than the Brunel mechanism, as one can see in Fig. 2a,c. Similarly, the influence of the bound-free-bound transitions for 0th harmonics are obviously negligible (a nearly DC field drives the electrons away, preventing recollisions), while that for the 3rd harmonic is estimated to be still few orders of magnitude below the bound-free ones. At $n > 3$, region III starts (Fig. 2a,c orange shading), where, according to our calculations, the bound-free-bound transition plays the dominant role. This can be seen from the nearly-exponential decay of the harmonic intensity as a function of harmonic order in the Drude model [12, 54], which is in contrast with the Coulomb and Yukawa cases, that show a more plateau-like structure. Finally, we note that the difference in harmonic intensity between the Coulomb and Yukawa calculations comes from the fact that the potential barrier in the Yukawa potential is wider than in the Coulomb case, which thus reduces the ionization probability.

Two-color field

Taking into account the above analysis, we focus only on region II (0th and 3rd order harmonic) where the Brunel mechanism is dominant. For the 2-color case, the 3rd harmonic is nearly circularly polarized in all of the calculations, owing to angular momentum selection rules. In contrast, the 0th harmonic is much closer to linear polarization. More importantly, we observe that the direction of the main polarization axis of the 0th harmonic for the case of the Yukawa potential and the Coulomb potential differ by $\phi \approx -10.0$ degree, which corresponds perfectly to the so-called ionization delay $\tau = \phi/\omega_0 \approx 74$ as calculated for hydrogen using the traditional attoclock technique [26]. Such ionization delay is caused by the dynamics of the electron in the Coulomb field and completely disappears in the short-range Yukawa potential. For sufficiently strong fields, this value approaches a constant independent on the field intensity and, in a first approximation, on the field shape. This is because it is determined only by the electron dynamics in a rather short time interval close to the field extrema.

To verify that the rotation of the polarization ellipse of the 0th order harmonic is indeed related to the ionization delay, we propose a description of the problem based on the Drude model which takes into account this ionization delay. Namely, we describe the radiation emitted by the bound-free transitions (Brunel harmonics) by

$$\mathbf{E}_r(t) = \mathbf{E}(t)\rho(t + \tau) \quad (1)$$

where τ is the ionization delay. We call this the “delayed Drude model”, since the free electron movement after ionization in the Coulomb field is replaced here by the movement *without* the Coulomb potential but delayed by the ionization time τ . In the model, τ is a parameter whose meaning and value lies outside the model itself; however, the validity of our approach and the interpretation of τ as a time delay, at least for the attoclock problem, can be proven (see Methods) using the analytical R-matrix theory [26, 55, 56] and is confirmed by our simulations below. It is also compatible with the Green-function approach [34, 39] (see Methods for details).

Equation 1 can be rewritten in the frequency domain as:

$$\mathbf{E}_{r,n} = \sum_j \mathbf{E}_j \rho_{n-j} e^{i(n-j)\omega_0\tau}, \quad (2)$$

where the free electron density ρ_x is an odd function of x , and \mathbf{E}_j is the j -th Fourier component of the pump field. In Jones vector notation and for the two-color field, the latter can be expressed as (see Methods): $\mathbf{E}_1 = (1, i)$, $\mathbf{E}_{-1} = (1, -i)$, $\mathbf{E}_2 = (1, i)$, $\mathbf{E}_{-2} = (1, -i)$. For the 0th-order we have thus: $\mathbf{E}_{r,0} = \mathbf{E}_1\rho_{-1} + \mathbf{E}_{-1}\rho_1 + \mathbf{E}_2\rho_{-2} + \mathbf{E}_{-2}\rho_2$, which leads to (see Methods):

$$\mathbf{E}_{r,0} \sim (\sin(\omega_0\tau), \cos(\omega_0\tau)). \quad (3)$$

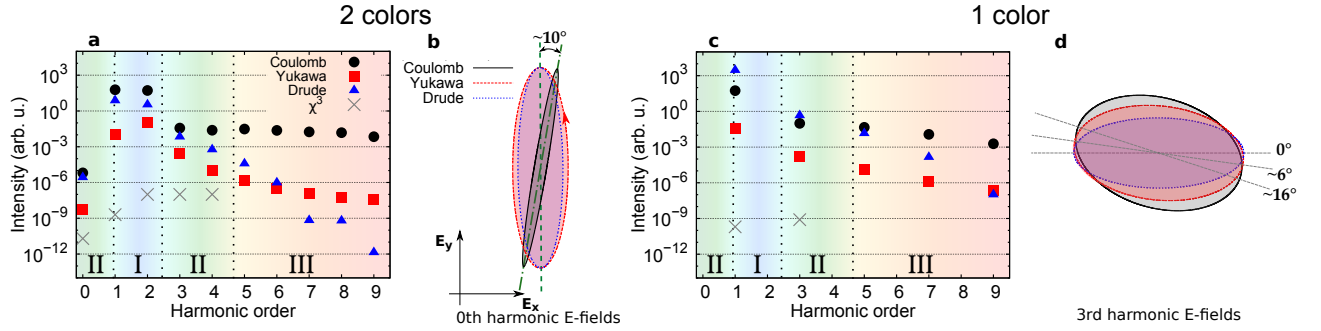


FIG. 2. The harmonic spectra (a,c) and the polarization states (b,d) of the TDSE simulation with Coulomb and Yukawa potentials as well as the simulation of the Drude model (without delay). In the two-color case, the field strength is $E_0 = 0.0375$ a.u. for both drivers and in the single-color case $E_0 = 0.07$ a.u. with an ellipticity of $\epsilon = 0.6$ along the y -direction. Both cases have a pulse duration of 20 fs. In (a,c) the results of a $\chi^{(3)}$ model are also presented. In (a,c) the regions I-III identify the different leading transition mechanisms: in I, the polarization state is determined by the pump, in II, by the bound-continuum whereas in III bound-continuum-bound and bound-bound transitions play the main role.

That is, the delayed Drude model predicts that for the case of zero ionization delay $\tau = 0$ the 0th harmonic is linearly polarized in the y -direction whereas for nonzero ionization time the polarization vector is rotated by $\omega_0\tau$ (see Fig. 1b). This model is well supported by the TDSE simulations (see Fig. 2b). For both the Drude model and the Yukawa cases, the major axis of the polarization ellipse of the 0th harmonic is along the y -direction. In contrast, for hydrogen, where the Coulomb potential is present, the ellipse rotates by ~ 10 degrees. Using Eq. (3), this value corresponds perfectly to the tunneling time delay $\tau \approx 74$ as given in [26].

The deviation from the zero ellipticity implied in Eq. (3) is well-explained by the fact that we consider not exactly a zero frequency but a tail of the 0th harmonic at around 100 THz (see Methods), and the ellipticity monotonously increases with the frequency. This explanation is corroborated by the agreement between the Drude model and the TDSE for the Yukawa potential. In contrast, the ellipticity of the 0th harmonic for the Coulomb potential is significantly less than the one of Yukawa, which we explain by the Coulomb focusing.

As one can see from Eq. (3), except for the ionization delay the polarization state of the 0th harmonic Eq. (3) does not depend on the particular temporal shape of $\rho(t)$. As we will see, for higher Brunel harmonics this is no longer the case.

Single-color field

In this section, we show that the 3rd harmonic may provide further information about the ionization dynamics. For the 2-color driver, the 3rd harmonic is circularly polarized, not allowing the definition of a polarization direction. This brings us to the idea of an even simpler pump configuration, namely the single-color elliptical pump (see Fig. 1c), which corresponds to the

pump field represented as: $\mathbf{E}_1 = (1, il)$, $\mathbf{E}_{-1} = (1, -il)$ where l is the ellipticity. In this case, the 0th harmonic is not generated, but the 3rd harmonic still lies in region II (see Fig. 2b), that is, the bound-free transitions dominate the atomic response. In this case, the Drude model from Eq. (2) gives us for the 3rd Brunel harmonic: $\mathbf{E}_{r,3} = \mathbf{E}_1\rho_2 + \mathbf{E}_{-1}\rho_4$, which translates to an electric field given by:

$$\mathbf{E}_{r,3} \sim (1 + r/2, il(1 - r/2)), \quad r = 2\rho_4 e^{2i\tau\omega_0} / \rho_2. \quad (4)$$

Eq. (4) shows that the polarization state of the 3rd harmonic depends critically on the 2nd and 4th harmonics of the ionization rate $\rho(t)$. This explains quite well the very different results for the ellipticity and polarization direction of different models (Drude and TDSE with Yukawa and Coulomb potentials), since the subcycle dynamics of the ionization in these cases is indeed expected to be different.

Fig. 3 shows the maps which allow to reconstruct the parameter r defined by Eq. (4) in terms of the polarization direction and ellipticity of the 3rd harmonic. We are interested in the dynamics of the ionization rate $W(t)$ and its harmonics W_n which for a small ρ are given by $W_n = in\omega_0\rho_n$. Eq. (4) implies thus that $W_4/W_2 = re^{-2i\tau\omega_0}$. To explain the results of the TDSE simulations one has to assume that not only r but also W_4/W_2 is a complex quantity. Its absolute value $|r|$ determines how sharp the ionization spike is. For instance, for the “absolutely sharp” ideal δ -function-like $W(t)$, $|r| = 1$. A smoother ionization process corresponds to a smaller $|r|$. Furthermore, to understand the meaning of the phase of r , we note that a time delay $W(t) \rightarrow W(t + \tau)$ induces in the frequency domain a delay-dependent phase shift $W_n \rightarrow W_n e^{in\omega_0\tau}$.

Our result shows that in addition to this spectral-phase shift, there must be an additional phase modification which is only present in higher harmonics. Both effects

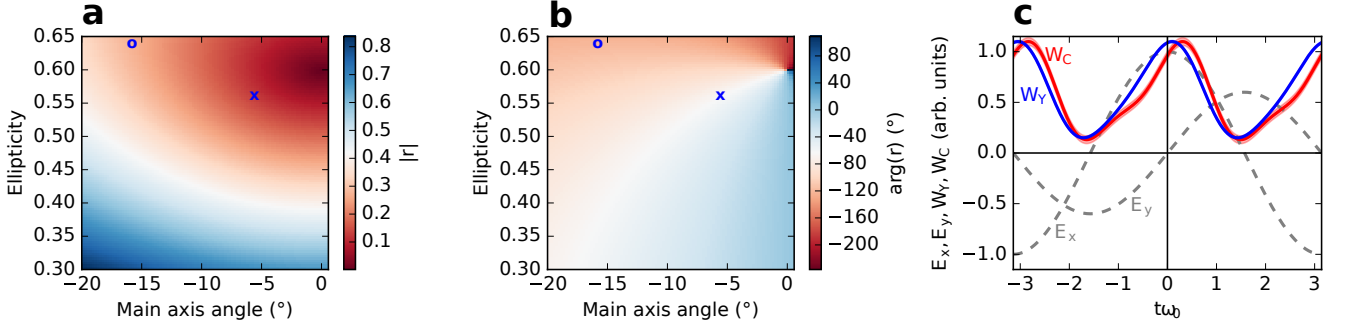


FIG. 3. (a,b) Reconstruction of $|r|$ (a) and $\arg(r)$ (b) from the polarization data of the 3rd harmonics, by numerically inverting Eq. (4). Circles and crosses show the particular data from Fig. 2d for the Coulomb and Yukawa potentials, correspondingly. In (c), the reconstruction of the ionization rate dynamics for the Coulomb (red line) and the Yukawa (blue line) potentials are shown, together with the pump electric field (dashed gray lines).

modify the ionization rate (represented by $\{W_n\}$) as:

$$W_0 \rightarrow W_0, W_2 \rightarrow W_2 e^{2i\omega_0\tau}, W_4 \rightarrow W_4 e^{4i\omega_0\tau + i\delta}, \dots \quad (5)$$

where δ , as it follows from the definitions above, is related to r as: $\delta = \arg(r) - 4\omega_0\tau$. It is easy to see that δ leads to an additional reshaping of $W(t)$ in respect to its time reflection $t \rightarrow -t$ with time zero being the maximum of $W(t)$.

Although the observation of 3rd harmonic provides only limited information about the ionization dynamics, it is already sufficient to reconstruct the dynamics with a fairly good level of precision. Indeed, we observe from our reconstruction that $|r|$ is quite small, namely $|r| = 0.14$ for the Yukawa and $|r| = 0.27$ for the Coulomb potential. It is reasonable to expect, that the next term in ionization is of the order of $|r|^2$ which gives us 7% uncertainty from unknown W_6 for the Coulomb potential and 2% for the Yukawa one, therefore we can neglect W_6 and the higher terms in the present case. Finally, the value of W_0 can be estimated from the ionization rate at the minimum of our elliptical field. Having this in mind and also using the known ionization delay $\tau \approx 74$ as, we are able to construct the ionization rate as a sum of harmonics W_0, W_2, W_4 with the corresponding amplitudes and phases. The result of the reconstruction is shown in Fig. 3c. One can see that the ionization for the Coulomb potential is not only time-shifted but also shows a certain asymmetry in respect to the ionization maximum. Reconstruction from the Yukawa potential still displays a reshaping of the ionization rate, albeit to an almost negligible extent. Thus, we were able to demonstrate that the capabilities of the proposed technique go beyond the mere delay measurement, and include the reconstruction of the deep-subcycle features of the ionization rate.

CONCLUSION

As a conclusion, we have shown that the low-frequency radiation during below-threshold ionization, despite its rather long period, is able to provide crucial information about attosecond-scale details of the electron ionization dynamics. In particular, we showed the possibility of an attoclock technique using the 0th-order Brunel harmonic in the case of a 2-color field. The attoclock translates one attosecond of ionization time delay to 0.1 degree of polarization emission ellipse rotation. Taking into account that the polarization can be determined with mrad precision, this is a promising mechanism for sub-attosecond time resolutions. Furthermore, we have shown that in the case of an 1-color driver the polarization and ellipticity of the 3rd Brunel harmonic is very sensitive to the temporal shape of the ionization step and allow its reconstruction, including a noticeable temporal asymmetry in the ionization delay. All this illustrates the promising capabilities of the proposed new tool, which allows to shed light at the ionization dynamics in the attosecond time scale – and even beyond it – with a setup that is much simpler than the electron-detection based ones. The potential of this method allows to extend it far beyond the ionization dynamics reconstruction in noble gases, to the solid state, where the electron-based attoclock performs poorly, allowing the study of the bound-bound transitions where attosecond-long delays were recently detected [57–59].

METHODS

Pump field in time and frequency representation

In general, we consider one-color field in the form:

$$E_x(t) = E_0 e^{-2 \ln 2 t^2 / \tau^2} \cos \omega_0 t, \quad (6)$$

$$E_y(t) = \epsilon E_0 e^{-2 \ln 2 t^2 / \tau^2} \sin \omega_0 t, \quad (7)$$

where, in our simulations, ω_0 corresponds to the wavelength 0.8 μm , $E_0 = 0.07$ au, the pulse duration is $\mathcal{T} = 20$ fs and the ellipticity is $\epsilon = 0.6$. For the two-color field we have

$$E_x(t) = -E_0 e^{-2 \ln 2 t^2 / \mathcal{T}^2} (\cos \omega_0 t + \cos 2\omega_0 t), \quad (8)$$

$$E_y(t) = E_0 e^{-2 \ln 2 t^2 / \mathcal{T}^2} (\sin \omega_0 t + \sin 2\omega_0 t), \quad (9)$$

with $\omega_0 = 0.8 \mu\text{m}$, $E_0 = 0.0375$ au, and $\mathcal{T} = 20$ fs.

In deriving the equations for the Brunel harmonics response, we used the Jones vector representation for the field harmonics $\mathbf{E}(t) = \sum_n \mathbf{E}_n e^{in\omega}$. The shape described in Eqs. (6)-(9), can be easily translated into \mathbf{E}_n . For instance, for an exemplary field $E_x = E_0 \cos(\omega_0 t)$, $E_y = E_0 \sin(\omega_0 t)$ we can easily obtain using the Euler formulas: $\mathbf{E}_1 = E_0/2 \cdot (1, 1/i)$, $\mathbf{E}_{-1} = E_0/2 \cdot (1, -1/i)$ where the first and second component of the vector are x and y components, respectively. In Results, we removed for simplicity the common factor $\pm E_0/2$.

TDSE simulations

Our TDSE equation has the well known form (we use atomic units across the article):

$$i\partial_t \psi(\mathbf{r}, t) = H\psi(\mathbf{r}, t), \quad H = (\mathbf{p} + \mathbf{A}(t))^2/2 + V(r), \quad (10)$$

where $\psi(\mathbf{r}, t)$ is the wavefunction of the electron depending on space \mathbf{r} (with $r \equiv |\mathbf{r}|$) and time t , H is the electron's Hamiltonian, with p being the momentum operator, $\mathbf{A}(t)$ the vector field potential of the external field, with the corresponding field strength $\mathbf{E}(t)$. The simulation box size used for the integration was 500 au. Simulations were repeated with the uniform and logarithmic spatial grid, with comparison to ensure the numerical convergence.

The response of the atom, \mathbf{E}_r was calculated as: $\mathbf{E}_r = g\partial_{tt}\mathbf{p} = g\partial_t\mathbf{j}$, where $\mathbf{p} = \langle \psi | \mathbf{r} | \psi \rangle$ is the atomic polarization, $|\psi\rangle$ is the electron wavefunction, $\mathbf{j} = \partial_t\mathbf{p}$ is the current assigned to \mathbf{p} , and g is the constant depending on the position of the observer, which we assume $g = 1$ for simplicity. In Fig. 2, the relevant quantities (polarization direction, ellipticity) were averaged around the frequencies $n\omega_0$ in the range $(0.9n\omega_0, 1.1n\omega_0)$ for n th harmonic except $n = 0$; Polarization direction and ellipticity being weighted with the intensity by averaging. For $n = 0$, because of our numerical limitations (huge box in time and space needed, together with the resolution of large number of angular harmonics makes it a very difficult task), we excluded extremely low frequencies $\omega < 0.25\omega_0$ from the analysis, thus restricting our predictions to the upper part of the THz frequency range. These frequencies still display a very good agreement with the calculations for the 0th harmonic for $\omega \rightarrow 0$.

From TDSE to the delayed Drude model.

In the framework of the analytic R-matrix approach [26, 55, 56] the electron wavefunction can be written as: $\psi(\mathbf{r}, t) = \sum_{t_s, \mathbf{p}} \langle \mathbf{r} | \mathbf{p} \rangle R_{\mathbf{p}} e^{iS(\mathbf{p}, t, t_s)}$, with $R_{\mathbf{p}}$ encodes the angular structure of the initial state, t_s is the (complex-valued) stationary time (see below), and $S = S_f + S_C$, $S_f = 1/2 \int_{t_s - i\kappa}^t (\mathbf{p} + \mathbf{A})^2 + I_p t_s$, $S_C = \int_{t_s - i\kappa}^t V(\tau) d\tau$, where $\kappa = \sqrt{2I_p}$ and I_p is the ionization potential. The ionization time t_s is inferred via the stationary phase approach from the equation $\partial_{t_s} S = 0$. t_s is different from the ionization time t_0 in a short range potential defined from $\partial_{t_0} S_f = 0$, and hereupon we express $\tau = \text{Re}(t_s - t_0)$. We note that for hydrogen, the value of τ can be obtained as a perturbation from the relation $\tau \partial_{t_s} S_f = \partial_{t_s} S_C$ as ≈ -74 as. By neglecting the term $\tau \partial_{t_0} S$ in the vicinity of t_0 we obtain that $S(t, \mathbf{p}, t') \approx S_f(t, \mathbf{p}, t') + C(t, \mathbf{p})$ with C being some constant in t' . This leads us to the following simplified problem to solve:

$\psi(\mathbf{r}, t) = \sum_{t_0, \mathbf{p}} \langle \mathbf{r} | \mathbf{p} \rangle e^{iS_f(\mathbf{p}, t, t_0 + \tau) + iC(t, \mathbf{p})}$. Furthermore, assuming that all electrons are created with $\mathbf{p} = 0$ making C an insignificant common phase, allowing to finally obtain the classical equation: $\mathbf{E}_r(t) \equiv \partial_t \mathbf{j} = \mathbf{E}(t)\rho(t)$ where $\rho(t) \approx \int_{-\infty}^t W(t' + \tau) dt'$ is the density of free electrons determined by the ionization rate $W(t)$ advanced by the time τ . In our simple theory for $W(t)$ we used the so called quasi-static formula [60].

We note that the delayed Drude model by itself does not fix the ionization time τ , it must be obtained from one other consideration, for instance the one presented above. We note however that this model is also compatible with the Green-function approach [34, 39] which predicts the small positive delays due to the nonzero values of initial velocity at the exit from the classically-forbidden region. In this case, introducing the delay into the Drude model is in fact an effective shift of the classical trajectory to negative exit times, so that at time $t = 0$ such shifted trajectory has already nonzero momentum. The value of the momentum of the classical trajectories at $t = 0$ is around 0.3 au and is in agreement with [34, 39]. Besides, our results on the 0th harmonic attoclock can be interpreted in this way, also confirming the approach in [34, 39] since the necessary τ shift for moderate fields for a Yukawa potential must be zero while being nonzero for the Coulomb one.

ACKNOWLEDGEMENTS

I.B., A.D. and U.M are thankful to Deutsche Forschungsgemeinschaft (DFG) (projects BA 4156/4-1, MO 850-19/1, MO 850-20/1) for financial support.

-
- [1] M. Hentschel, R. Kienberger, Ch Spielmann, G. A. Reider, N. Milosevic, T. Brabec, P. Corkum, U. Heinzmann, M. Drescher, and F. Krausz, "Attosecond metrology," *Nature* **414**, 509 (2001), article.
 - [2] P. B. Corkum and Ferenc Krausz, "Attosecond science," *Nature Phys.* **3**, 381 (2007).
 - [3] E. Goulielmakis, V. S. Yakovlev, A. L. Cavalieri, M. Uiberacker, V. Pervak, A. Apolonski, R. Kienberger, U. Kleineberg, and F. Krausz, "Attosecond control and measurement: Light-wave electronics," *Science* **317**, 769–775 (2007).
 - [4] T. T. Luu, M. Garg, S. Yu Kruchinin, A. Moulet, M. Th. Hassan, and E. Goulielmakis, "Extreme ultraviolet high-harmonic spectroscopy of solids," *Nature* **521**, 498 (2015).
 - [5] C. I. Blaga, F. Catoire, P. Colosimo, G. Paulus, H. G. Muller, P. Agostini, and L. F. DiMauro, "Strong-field photoionization revisited," *Nature Phys.* **5**, 335–338 (2009).
 - [6] O. Smirnova, Y. Mairesse, S. Patchkovskii, N. Dudovich, D. Villeneuve, P. Corkum, and M. Yu. Ivanov, "High harmonic interferometry of multi-electron dynamics in molecules," *Nature* **460**, 972 (2009).
 - [7] T.-M. Yan, S. V. Popruzhenko, M. J. J. Vrakking, and D. Bauer, "Low-energy structures in strong field ionization revealed by quantum orbits," *Phys. Rev. Lett.* **105**, 253002 (2010).
 - [8] S. Haessler, J. Caillat, W. Boutu, C. Giovanetti-Teixeira, T. Ruchon, T. Auguste, Z. Diveki, P. Breger, A. Maquet, B. Carré, *et al.*, "Attosecond imaging of molecular electronic wavepackets," *Nature Phys.* **6**, 200–206 (2010).
 - [9] Y. Huismans, A. Rouzée, A. Gijsbertsen, J. H. Jungmann, A. S. Smolkowska, P. S. W. M. Logman, F. Lépine, C. Cauchy, S. Zamith, T. Marchenko, J. M. Bakker, G. Berden, B. Redlich, A. F. G. van der Meer, H. G. Muller, W. Vermin, K. J. Schafer, M. Spanner, M. Yu. Ivanov, O. Smirnova, D. Bauer, S. V. Popruzhenko, and M. J. J. Vrakking, "Time-

- resolved holography with photoelectrons,” *Science* **331**, 61–64 (2011).
- [10] A. Kästner, U. Saalmann, and Jan M. Rost, “Electron-energy bunching in laser-driven soft recollisions,” *Phys. Rev. Lett.* **108**, 033201 (2012).
- [11] F. Lépine, M. Y. Ivanov, and M. J. J. Vrakking, “Attosecond molecular dynamics: fact or fiction?” *Nature Photon.* **8**, 195–204 (2014).
- [12] F. Brunel, “Harmonic generation due to plasma effects in a gas undergoing multiphoton ionization in the high-intensity limit,” *J. Opt. Soc. Am. B* **7**, 521–526 (1990).
- [13] A. J. Verhoef, A. V. Mitrofanov, E. E. Serebryannikov, D. V. Kartashov, A. M. Zheltikov, and A. Baltuška, “Optical detection of tunneling ionization,” *Phys. Rev. Lett.* **104**, 163904 (2010).
- [14] I. Babushkin, C. Brée, Ch. M. Dietrich, A. Demircan, U. Morgner, and A. Husakou, “Terahertz and higher-order Brunel harmonics: from tunnel to multiphoton ionization regime in tailored fields,” *J. Mod. Opt.* **64**, 1078–1087 (2017).
- [15] T. Balciunas, A. J. Verhoef, A. V. Mitrofanov, G. Fan, E. E. Serebryannikov, M. Y. Ivanov, A. M. Zheltikov, and A. Baltuška, “Optical and THz signatures of sub-cycle tunneling dynamics,” *Chemical Physics* **414**, 92–99 (2013).
- [16] T. Bartel, P. Gaal, K. Reimann, M. Woerner, and T. Elsaesser, “Generation of single-cycle THz transients with high electric-field amplitudes,” *Opt. Lett.* **30**, 2805–2807 (2005).
- [17] M. Kieß, Torsten Löffler, M. D. Thomson, R. Dörner, H. Gimpel, K. Zrost, T. Ergler, R. Moshhammer, U. Morgner, J. Ullrich, *et al.*, “Determination of the carrier-envelope phase of few-cycle laser pulses with terahertz-emission spectroscopy,” *Nature Phys.* **2**, 327–331 (2006).
- [18] K. Reimann, “Terahertz radiation: A table-top source of strong pulses,” *Nat Photon* **2**, 596–597 (2008).
- [19] K. Y. Kim, A. J. Taylor, J. H. Glowina, and G. Rodriguez, “Coherent control of terahertz supercontinuum generation in ultrafast laser-gas interactions,” *Nature Photon.* **2**, 605–609 (2008).
- [20] T. Kampfrath, K. Tanaka, and K. A. Nelson, “Resonant and nonresonant control over matter and light by intense terahertz transients,” *Nature Photon.* **7**, 680–690 (2013).
- [21] M. Woerner, W. Kuehn, P. Bown, K. Reimann, and Th. Elsaesser, “Ultrafast two-dimensional terahertz spectroscopy of elementary excitations in solids,” *New J. Phys.* **15**, 025039 (2013).
- [22] P. M. Kraus, B. Mignolet, D. Baykusheva, A. Rupenyan, L. Horný, E. F. Penka, G. Grassi, O. I. Tolstikhin, J. Schneider, F. Jensen, *et al.*, “Measurement and laser control of attosecond charge migration in ionized iodoacetylene,” *Science* **350**, 790–795 (2015).
- [23] P. Eckle, M. Smolarski, Ph. Schlup, J. Biegert, A. Staudte, M. Schöffler, H. G. Muller, R. Dörner, and U. Keller, “Attosecond angular streaking,” *Nature Phys.* **4**, 565 (2008).
- [24] P. Eckle, A. N. Pfeiffer, C. Cirelli, A. Staudte, R. Dörner, H. G. Muller, M. Büttiker, and U. Keller, “Attosecond ionization and tunneling delay time measurements in helium,” *Science* **322**, 1525–1529 (2008).
- [25] D. Shafir, H. Soifer, B. D. Bruner, M. Dagan, Y. Mairesse, S. Patchkovskii, M. Y. Ivanov, O. Smirnova, and N. Dudovich, “Resolving the time when an electron exits a tunnelling barrier,” *Nature* **485**, 343–346 (2012).
- [26] L. Torlina, F. Morales, J. Kaushal, I. Ivanov, A. Kheifets, A. Zielinski, A. Scrinzi, H. G. Muller, S. Sukiasyan, M. Ivanov, *et al.*, “Interpreting attoclock measurements of tunnelling times,” *Nature Phys.* **11**, 503–508 (2015).
- [27] R. Kienberger, E. Goulielmakis, M. Uiberacker, A. Baltuška, V. Yakovlev, F. Bammer, A. Scrinzi, Th. Westerwalbesloh, U. Kleineberg, U. Heinzmann, *et al.*, “Atomic transient recorder,” *Nature* **427**, 817 (2004).
- [28] A. N. Pfeiffer, C. Cirelli, M. Smolarski, D. Dimitrovski, M. Abu-samha, L. B. Madsen, and U. Keller, “Attoclock reveals natural coordinates of the laser-induced tunnelling current flow in atoms,” *Nature Phys.* **8**, 76 (2011).
- [29] A. S. Landsman, M. Weger, J. Maurer, R. Boge, A. Ludwig, S. Heuser, C. Cirelli, L. Gallmann, and U. Keller, “Ultrafast resolution of tunneling delay time,” *Optica* **1**, 343–349 (2014).
- [30] M. Han, P. Ge, Y. Shao, Q. Gong, and Y. Liu, “Attoclock photoelectron interferometry with two-color corotating circular fields to probe the phase and the amplitude of emitting wave packets,” *Phys. Rev. Lett.* **120**, 073202 (2018).
- [31] M. Büttiker and R. Landauer, “Traversal time for tunneling,” *Phys. Rev. Lett.* **49**, 1739–1742 (1982).
- [32] A. M. Steinberg, P. G. Kwiat, and R. Y. Chiao, “Measurement of the single-photon tunneling time,” *Phys. Rev. Lett.* **71**, 708–711 (1993).
- [33] D. Sokolovski, S. Brouard, and J. N. L. Connor, “Traversal-time wave-function analysis of resonance and nonresonance tunneling,” *Phys. Rev. A* **50**, 1240 (1994).
- [34] E. Yakaboylu, M. Klaiber, and K. Z. Hatsagortsyan, “Wigner time delay for tunneling ionization via the electron propagator,” *Phys. Rev. A* **90**, 012116 (2014).
- [35] A. S. Landsman and U. Keller, “Attosecond science and the tunnelling time problem,” *Phys. Rep.* **547**, 1–24 (2015).
- [36] J. Kaushal, F. Morales, L. Torlina, M. Ivanov, and O. Smirnova, “Spin-orbit Larmor clock for ionization times in one-photon and strong-field regimes,” *Journal of Physics B: Atomic, Molecular and Optical Physics* **48**, 234002 (2015).
- [37] H. Ni, U. Saalmann, and J.-M. Rost, “Tunneling ionization time resolved by backpropagation,” *Phys. Rev. Lett.* **117**, 023002 (2016).
- [38] N. Teeny, E. Yakaboylu, H. Bauke, and C. H. Keitel, “Ionization time and exit momentum in strong-field tunnel ionization,” *Phys. Rev. Lett.* **116**, 063003 (2016).
- [39] N. Camus, E. Yakaboylu, L. Fechner, M. Klaiber, M. Laux, Y. Mi, K. Z. Hatsagortsyan, T. Pfeifer, C. H. Keitel, and R. Moshhammer, “Experimental evidence for quantum tunneling time,” *Phys. Rev. Lett.* **119**, 023201 (2017).
- [40] C. I. Blaga, J. Xu, A. D. DiChiara, E. Sistrunk, K. Zhang, P. Agostini, T. A. Miller, L. F. DiMauro, and C. D. Lin, “Imaging ultrafast molecular dynamics with laser-induced electron diffraction,” *Nature* **483**, 194 (2012).
- [41] J. Zhao and M. Lein, “Determination of ionization and tunneling times in high-order harmonic generation,” *Phys. Rev. Lett.* **111**, 043901 (2013).
- [42] E. W. Larsen, S. Carlström, E. Lorek, Ch. M. Heyl, D. Paleček, K. J. Schafer, A. LHuillier, D. Zigmantas, and J. Mauritson, “Sub-cycle ionization dynamics revealed by trajectory resolved, elliptically-driven high-order harmonic generation,” *Sci. Rep.* **6**, 39006 (2016).
- [43] Xinhua Xie, Marlene Wickenhauser, W. Boutu, H. Merdji, P. Salieres, and Armin Scrinzi, “Subcycle dynamics in the laser ionization of molecules,” *Phys. Rev. A* **76**, 023426 (2007).
- [44] R. Murray, M. Spanner, S. Patchkovskii, and M. Y. Ivanov, “Tunnel ionization of molecules and orbital imaging,” *Phys. Rev. Lett.* **106**, 173001 (2011).
- [45] W. Chen, S. Zhang, and X. Long, “Polarisation control through an optical feedback technique and its application in precise measurements,” *Sci. Rep.* **3** (2013).
- [46] Y. Ikebe and R. Shimano, “Characterization of doped silicon in low carrier density region by terahertz frequency faraday effect,” *Appl. Phys. Lett.* **92**, 012111 (2008).
- [47] Natsuki Nemoto, Takuya Higuchi, Natsuki Kanda, Kuniaki Konishi, and Makoto Kuwata-Gonokami, “Highly precise and accurate terahertz polarization measurements based on electro-optic sampling with polarization modulation of probe pulses,” *Opt. Expr.* **22**, 17915–17929 (2014).
- [48] A. Jablonski, P. Mrozek, G. Gergely, M. Menhyard, and A. Sulyok, “The inelastic mean free path of electrons in some semiconductor compounds and metals,” *Surf. Interf. Anal.* **6**, 291–294 (1984).
- [49] A. L. Cavalieri, N. Müller, Th. Uphues, V. S. Yakovlev, A.

- Baltuška, B. Horvath, B. Schmidt, L. Blümel, R. Holzwarth, S. Hendel, *et al.*, “Attosecond spectroscopy in condensed matter,” *Nature* **449**, 1029 (2007).
- [50] C. Lemell, B. Solleder, K. Tókési, and J. Burgdörfer, “Simulation of attosecond streaking of electrons emitted from a tungsten surface,” *Phys. Rev. A* **79**, 062901 (2009).
- [51] K. T. Kim, D. M. Villeneuve, and P. B. Corkum, “Manipulating quantum paths for novel attosecond measurement methods,” *Nature Photon.* **8**, 187 (2014).
- [52] S. Patchkovskii and H. G. Muller, “Simple, accurate, and efficient implementation of 1-electron atomic time-dependent schrödinger equation in spherical coordinates,” *Computer Phys. Commun.* **199**, 153–169 (2016).
- [53] Ch. Köhler, R. Guichard, E. Lorin, S. Chelkowski, A. D. Bandrauk, L. Bergé, and S. Skupin, “Saturation of the nonlinear refractive index in atomic gases,” *Phys. Rev. A* **87**, 043811 (2013).
- [54] U. Sapaev, A. Husakou, and J. Herrmann, “Combined action of the bound-electron nonlinearity and the tunnel-ionization current in low-order harmonic generation in noble gases,” *Opt. Expr.* **21**, 25582–25591 (2013).
- [55] L. Torlina and O. Smirnova, “Time-dependent analytical r-matrix approach for strong-field dynamics. I. One-electron systems,” *Phys. Rev. A* **86**, 043408 (2012).
- [56] L. Torlina, M. Ivanov, Z. B. Walters, and O. Smirnova, “Time-dependent analytical r-matrix approach for strong-field dynamics. II. Many-electron systems,” *Phys. Rev. A* **86**, 043409 (2012).
- [57] M. Hofmann, J. Hyyti, S. Birkholz, M. Bock, S. K. Das, R. Grunwald, M. Hoffmann, T. Nagy, A. Demircan, M. Jupé, D. Ristau, U. Morgner, C. Brée, M. Woerner, T. Elsaesser, and G. Steinmeyer, “Noninstantaneous polarization dynamics in dielectric media,” *Optica* **2**, 151–157 (2015).
- [58] A. Sommer, E. M. Bothschafter, S. A. Sato, C. Jakubeit, T. Latka, O. Razskazovskaya, H. Fattahi, M. Jobst, W. Schweinberger, V. Shirvanyan, *et al.*, “Attosecond nonlinear polarization and light-matter energy transfer in solids,” *Nature* **534**, 86 (2016).
- [59] M. Th. Hassan, T. T. Luu, A. Moulet, O. Razskazovskaya, P. Zhokhov, M. Garg, N. Karpowicz, A. M. Zheltikov, V. Pervak, Ferenc Krausz, *et al.*, “Optical attosecond pulses and tracking the nonlinear response of bound electrons,” *Nature* **530**, 66 (2016).
- [60] M. V. Ammosov, N. V. Delone, and V. P. Krainov, “Tunnel ionization of complex atoms and of atomic ions in an alternating electromagnetic field,” *SovietPhys. JETP* **64**, 1191 (1986).